

# Local Environment of Electrons Trapped at the MgO Surface: Spin Density on the Oxygen Ions from $^{17}\text{O}$ Hyperfine Coupling Constants

Mario Chiesa,<sup>†</sup> Paola Martino,<sup>†</sup> Elio Giamello,<sup>\*,†</sup> Cristiana Di Valentin,<sup>‡</sup>  
Annalisa del Vitto,<sup>‡</sup> and Gianfranco Pacchioni<sup>‡</sup>

Dipartimento di Chimica IFM, Università di Torino and Unità INFM di Torino Università,  
via P. Giuria 7, 10125 Torino, Italy and Dipartimento di Scienza dei Materiali,  
Università di Milano-Bicocca, Via R. Cozzi, 53–20125, Milano, Italy.

Received: January 19, 2004; In Final Form: May 24, 2004

The nature of electron traps at the surface of polycrystalline MgO is analyzed for the first time in terms of interaction of the electron spin with the nuclear spin of the  $^{17}\text{O}$  anions of the surface. MgO crystals enriched in the  $^{17}\text{O}$  isotope have been prepared and the corresponding hyperfine coupling constants have been measured in EPR spectra. The trapped electrons are produced by exposure of the samples to  $\text{H}_2$  followed by UV irradiation, with consequent production of paramagnetic  $(\text{H}^+)(\text{e}^-)$  centers. The EPR spectrum shows a multiplet structure with two main sextets separated by 51 and 10 G, respectively, due to the interaction of the unpaired electron with two nonequivalent  $^{17}\text{O}$  nuclei. The results are interpreted based on accurate quantum chemical calculations. It is suggested that the paramagnetic centers observed correspond to  $(\text{H}^+)(\text{e}^-)$  pairs formed at step sites of the MgO surface.

## 1. Introduction

Trapped electrons in insulating materials, also known as F or color centers, are a milestone of solid-state physics and chemistry<sup>1</sup> and have been recently enjoying a wealth of renewed interest due to the possibility of obtaining stoichiometric excess electron doping, which leads to new classes of materials generally known as inorganic electrides.<sup>2,3</sup>

Under some circumstances electron trapping and excess electron doping can be restricted to the surface of insulating materials, leading to “electron rich” surfaces.<sup>4</sup> In this case the trapped electrons, being localized at a solid–gas interface, are extremely reactive and can act as powerful reducing agents.<sup>5,6</sup> Furthermore they are excellent probes of the local environment of the surface defective sites that act as electron trapping centers. The influence of structural imperfections in driving the chemical and physical properties of solid surfaces is well recognized and it is clear that defects are involved in electron trapping phenomena. However, while localized excess electrons in the bulk of ionic solids are generally well understood based on the classical de Boer’s model (an electron trapped in an anion vacancy),<sup>7,8</sup> our understanding of the nature of the sites responsible for electron trapping at solid surfaces or interfaces lags somewhat behind that of bulk crystals. Such knowledge is crucial in order to fully appreciate and rationalize the surface chemistry of the materials under investigation but is also intrinsically important for the general problem of charge carriers stabilization in solids.<sup>2,9</sup>

For the past few years we have been engaged in the investigation of excess localized electrons at the surface of polycrystalline metal oxides such as MgO.<sup>10–12</sup> The generation

of surface- trapped electrons on the totally dehydrated (hydroxyl free) MgO surface can be obtained by UV irradiation of the solid in the presence of molecular hydrogen.<sup>4</sup>  $\text{H}_2$  is believed to dissociate heterolitically at some specific sites with formation of an  $(\text{H}^+)(\text{H}^-)$  pair.<sup>13,14</sup> Under UV irradiation, neutral H atoms are desorbed leaving on the surface a trapped electron near an adsorbed proton,  $(\text{H}^+)(\text{e}^-)$ . Other trapped electrons are formed by the successive ionization of these H atoms at different surface sites that can be indicated in general as  $(\text{H}^+)(\text{e}^-)$ . It is important to note that these new centers, being obtained by dissociation of H atoms into  $\text{H}^+$  (bound at an  $\text{O}^{2-}$  ion) and  $\text{e}^-$  (stabilized at  $\text{Mg}^{2+}$  cations) are globally neutral and are not necessarily associated with the existence of oxygen vacancies.<sup>14</sup>

Major advances in understanding the nature of the electron-trapping sites have been possible through the successful combination of electron magnetic resonance techniques (EPR/ENDOR) and theoretical calculations.<sup>4,14,15</sup> EPR spectroscopy is an extremely powerful tool that allows one to monitor with high accuracy the distribution of the spin density in the surroundings of the trapping site, enabling a microscopic investigation of the neighborhood of the defect. These data can be directly compared with values obtained by ab initio quantum chemical modeling. This combined approach prompted us to propose specific models of the surface color centers mainly based on the  $^{25}\text{Mg}$  hyperfine tensor (the  $^{25}\text{Mg}$  nuclide,  $I = 5/2$ , has a natural abundance of about 10%).<sup>4,11,14</sup> Although some details of the nature of the trapping sites are still somewhat elusive, these can be interpreted in terms of potential wells constituted by different arrangements of  $\text{Mg}^{2+}$ , and even single  $\text{Mg}^{2+}$ , cations.<sup>16</sup> A full description of the unpaired electron spin distribution requires, however, one to monitor the hyperfine interaction with the oxygen anions that are part of the defective site. This can be done by enhancing the  $^{17}\text{O}$  ( $I = 5/2$ ) isotope concentration ( $^{16}\text{O}$  has nuclear spin  $I = 0$ ).

ESR and ENDOR spectroscopies have been used in the past<sup>17</sup> to investigate the  $\text{F}^+$  center (an electron trapped in an oxygen

\* Prof. Elio Giamello, Dipartimento di Chimica I. F. M., Via Giuria 9 - 10125 Torino Italy. Tel ++39-011-6707574; fax ++39-011-6707855; e-mail elio.giamello@unito.it.

<sup>†</sup> Dipartimento di Chimica IFM, Università di Torino and Unità INFM di Torino Università

<sup>‡</sup> Dipartimento di Scienza dei Materiali, Università di Milano-Bicocca

vacancy) in the bulk of MgO crystals enriched in the  $^{17}\text{O}$  isotope. In the present paper we show that corresponding data for the surface electron trapping sites can be obtained by labeling the oxide  $\text{O}^{2-}$  ions of the surface with  $^{17}\text{O}$ . This was done by hydration and dehydration cycles of the oxide with  $^{17}\text{O}$ -enriched  $\text{H}_2\text{O}$ . For the first time, the hyperfine parameters related to the  $(e^-)-(^{17}\text{O})$  magnetic interaction have been determined, thus completing the description of the spin density distribution of the surface electron trapping sites. The experimental data are compared and analyzed in the light of state of the art quantum chemical calculations.

## 2. Methods

**2.a. Experimental Details.** High-surface-area polycrystalline MgO has been prepared by slow decomposition of  $\text{Mg}(\text{OH})_2$  in a vacuum as described elsewhere.<sup>4,16</sup> The MgO powder was activated at 1173 K to remove impurities and then the surface was rehydrated, exposing the solid to vapor pressure of  $\text{H}_2^{17}\text{O}$  (86% isotopic enrichment supplied by Icon Services, NJ). The solid was then reactivated at 1173 K and surface excess electrons were generated by UV irradiation under an  $\text{H}_2$  atmosphere (10 mbar). UV irradiation of the sample was carried out at 77 K. After 15 min of irradiation, the sample develops a blue coloration, indicating the formation of surface color centers.

A 500-W *Oriel Instruments* UV lamp, incorporating an Hg/Xe arc lamp (250 nm to > 2500 nm), was used for all irradiations, in conjunction with a water filter. The UV output below 280 nm accounts for only 4 to 5% of the total lamp output.

EPR spectra were recorded at 298 K on a Bruker EMX spectrometer operating at X-band frequencies and equipped with a cylindrical cavity operating at a 100-kHz field modulation. The spectra have been recorded at 1-mW microwave power. The EPR computer simulations were obtained using the SIM32 program developed by Prof. Z. Sojka (Jagiellonian University, Cracow).<sup>18</sup>

**2.b. Computational Details.** The spin properties of the trapped electrons, and in particular the hyperfine interaction of the electron spin with the nuclear spin of the  $^{17}\text{O}$ ,  $^{25}\text{Mg}$ , and  $^1\text{H}$  nuclides, has been determined by computing the electronic structure of the defect centers with the help of embedded cluster models. The calculations were performed at the density functional theory (DFT) level using the gradient-corrected Becke's three parameters hybrid exchange functional<sup>19</sup> in combination with the correlation functional of Lee et al.<sup>20</sup> (B3LYP).

The hyperfine spin-Hamiltonian,  $\mathbf{H}_{\text{hfc}} = \mathbf{S} \cdot \mathbf{A} \cdot \mathbf{I}$ , is given in terms of the hyperfine matrix  $\mathbf{A}$  which describes the coupling between the electron and the nuclear spins.<sup>21</sup> The components of  $\mathbf{A}$  can be represented as the sum of an isotropic part,  $a_{\text{iso}}$ , related to the Fermi contact term, and the matrix  $\mathbf{B}$  which represents the "classical" dipolar interaction between two magnetic (electron and nuclear) moments. Typical anisotropic interactions can be observed when the unpaired electron is in directional orbitals such as p, d, f, etc. The  $\mathbf{A}$  tensor can therefore be represented in matrix notation as  $\mathbf{A} = a_{\text{iso}} + \mathbf{B}$ .

The MgO surface has been simulated by clusters embedded in an array of about 900 polarizable classical ions (shell model) surrounded by a matrix of about 3000 point charges.<sup>22</sup> Four kinds of electron traps have been considered. Three correspond to a  $(\text{H}^+)(e^-)$  pair formed in correspondence with different morphological defects, a step, a reverse corner (RC), and a corner. The clusters used,  $[\text{Mg}_{12}\text{O}_{13}(\text{H})]_{\text{step}}$ ,  $[\text{Mg}_{17}\text{O}_{17}(\text{H})]_{\text{RC}}$ , and  $[\text{Mg}_4\text{O}_4(\text{H})]_{\text{corner}}$ , are globally neutral. The fourth case is that of a paramagnetic oxygen vacancy at a terrace site with a proton

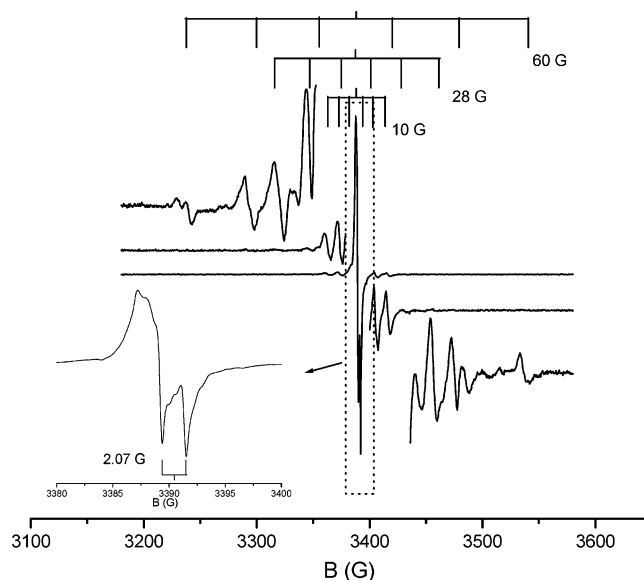


**Figure 1.** EPR spectrum of trapped electron centers on the surface of polycrystalline MgO. The stick diagrams refer to the three  $^{25}\text{Mg}$  hyperfine patterns. In the inset the hyperfine doublet relative to the interaction between the trapped electrons and the nearby proton is evidenced.

adsorbed in the vicinity. For historical reasons,<sup>4</sup> this center is called  $\text{F}_5(\text{H})^+$  although the corresponding cluster model carries a +2 net charge. In fact, the system consists of a paramagnetic  $\text{F}_5^+$  center with an adsorbed proton,  $\text{H}^+$ , and the final formula is  $[\text{Mg}_{17}\text{O}_{16}(\text{H})]^{2+}$ .

Particular attention has been given to the basis sets used to reproduce the hyperfine interactions. The geometrical optimization has been performed using the 6-31G basis set on all Mg and O ions and the 6-311+G\*\* on H,<sup>23,24</sup> but the calculations of the hyperfine coupling constants (hfcc) have been done using much more flexible basis sets, 6-311+G\* on Mg, and EPR-II on O and on H. The EPR-II basis has been specifically designed to accurately reproduce the hfcc of O-containing radicals.<sup>25</sup> For the  $\text{F}_5(\text{H})^+$  center only the Mg ions nearest to the vacancy have been treated with the 6-311+G\* basis, while for the other Mg cations we used the 6-31G basis. It should be mentioned that the  $a_{\text{iso}}$  and  $B$  values depend also, to some extent, on the choice of the exchange correlation functional. This aspect has been discussed in detail by Barone,<sup>25</sup> who has shown that in general, and in particular for  $^{17}\text{O}$ , the B3LYP functional used here gives the best agreement with the experiment. A more subtle problem is that trapped electrons and holes in insulators are not always properly described at the DFT level, since this approach tends to exaggerate the delocalized nature of unpaired electrons.<sup>26</sup> Hybrid functionals, such as the B3LYP, seem to provide accurate answers in several cases. However, in the comparison of theory with experiment one should not underestimate the importance of these aspects on the final computed values. The calculations have been performed using the Guess code<sup>22</sup> interfaced with the Gaussian98 program package.<sup>27</sup>

## 3. Results

**3.a. Experiments.** Before showing the results relative to the  $^{17}\text{O}$  enriched system, we briefly report the relevant data concerning the surface color centers generated on high surface area  $\text{Mg}^{16}\text{O}$ . Figure 1 shows the EPR spectrum of  $\text{Mg}^{16}\text{O}$  UV irradiated at 77 K in an  $\text{H}_2$  atmosphere. After irradiation the sample develops an intense blue color that is immediately bleached if a reactive gas such as  $\text{O}_2$  is admitted into the cell,

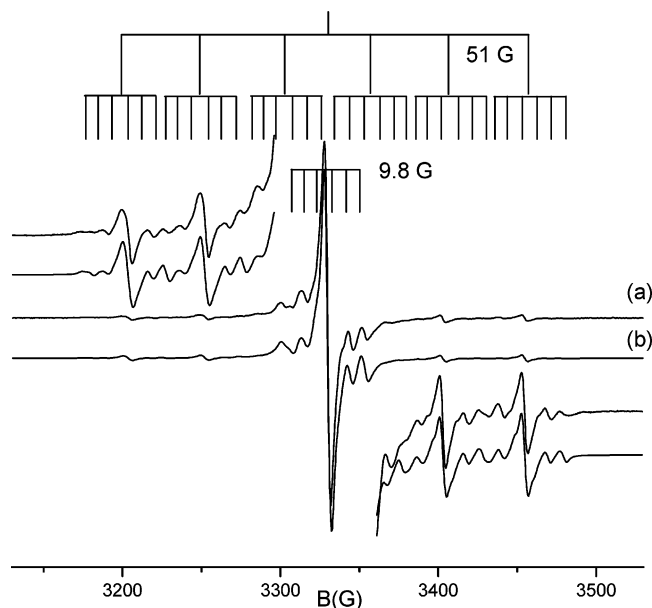


**Figure 2.** EPR spectrum of surface trapped electron centers on  $^{17}\text{O}$  enriched MgO. (a) Experimental (b) simulated spectrum. The stick diagrams indicate the two hyperfine patterns relative to  $^{17}\text{O}$  nuclei.

proving the surface nature of the trapped electron centers. The spectrum is dominated by a species with axial symmetry that resonates close to the free-electron  $g$  value ( $g_{\perp} = 1.9996$ ,  $g_{\parallel} = 2.0014$ ). The spectrum is also characterized by a doublet hyperfine splitting of 2.07 G (inset in Figure 1) known to arise from a magnetic interaction between the unpaired electron and the H atom of a neighboring OH group.<sup>4</sup> A second important feature is represented by a sextet hyperfine structure with an  $\approx 10$  G coupling that is outlined in Figure 1 with the aid of a stick diagram. The low intensity of this sextet reflects the low natural abundance (10.13%) of  $^{25}\text{Mg}^{2+}$  isotopes ( $I = 5/2$ ). By recording the spectrum in conditions of over-amplification and over-modulation, two additional and less intense sextet hyperfine features due to  $^{25}\text{Mg}^{2+}$  can be observed as recently reported by some of us.<sup>16</sup> These two low-intensity sextets are identified in Figure 1 by stick diagrams and the coupling constants are of about 60 and 28 G respectively. These two hyperfine features, together, account for about 20% of the entire spectrum and arise from two different paramagnetic centers. One, characterized by the 60-G hyperfine sextet, has been recently assigned<sup>16</sup> to electrons and protons bound at MgO corner sites and referred to as the  $\text{MgO}_{\text{corner}}(\text{H}^+)(\text{e}^-)$  center. The other, with a 28-G coupling constant, is constituted by an array of  $\text{Mg}^{2+}$  ions and its nature will be preliminarily discussed below and addressed in detail in a forthcoming paper.<sup>28</sup>

To obtain a complete description of the unpaired electron spin density and acquire extra data for the validation of the proposed models, information is needed on the hyperfine coupling with the anions in the surrounding of the trapping site. This has been done by enriching the surface with  $^{17}\text{O}$  as reported in the Experimental Section. The spectrum obtained after UV irradiation of the sample in  $\text{H}_2$  atmosphere, under the same conditions reported before, is shown in Figure 2a. The spectrum is dominated by an intense symmetrical line centered at  $g = 1.9995$  with a line width of about 5 G, and shows the trace of a new hyperfine structure absent in the spectrum of Figure 1 and therefore due to  $^{17}\text{O}$ . To the best of our knowledge the spectrum in Figure 2 represents the first example of the use of  $^{17}\text{O}$  to label the surface ions of an oxide leading to a resolved EPR spectrum. The increase in line width with respect to the

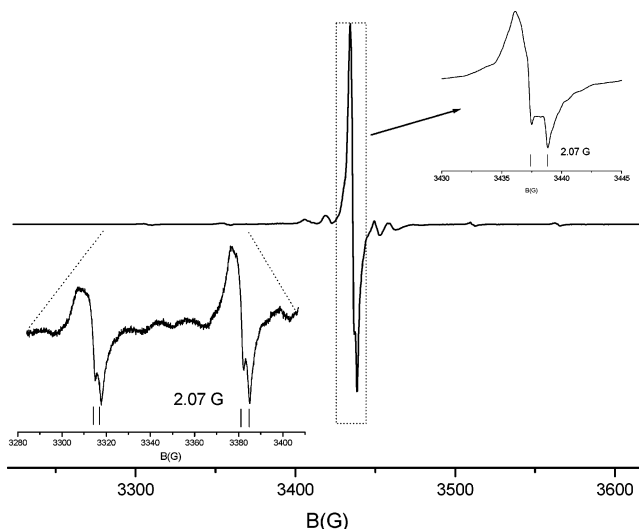


**Figure 3.** EPR spectrum of surface trapped electron centers on a sample with low  $^{17}\text{O}$  enrichment. The two insets show the characteristic hyperfine doublet due to the vicinal proton (see text for explanation).

$\text{Mg}^{16}\text{O}$  sample can be ascribed to the heterogeneous broadening induced by the presence of  $^{17}\text{O}$  nuclei and prevents from observing both the  $g$  anisotropy and the proton hyperfine coupling of the signal which are evident in Figure 1. The latter point has been demonstrated by an “ad-hoc” experiment on a sample with a reduced  $^{17}\text{O}$  enrichment obtained by contacting the surface with a lower amount of isotopically enriched water. Activating the sample and generating the trapped electrons in the usual way we obtained the spectrum reported in Figure 3. In this spectrum both the central line and the six main  $^{17}\text{O}$  hyperfine features show the coupling with the proton at 2.07 G confirming that the spectrum reported in Figure 2a is heterogeneously broadened.

The hyperfine structure visible in Figure 2a is based on two main independent sextets separated by 51 and 9.8 G respectively (stick diagram in the figure) and by a third less-intense structure consisting of 6 sextets with 9.8-G separation (36 lines in total), each one of them centered on one of the lines of the 51-G structure. The new hyperfine structure is due to the interaction of unpaired electrons with the  $^{17}\text{O}$  nuclei and is not related to the far weaker  $^{25}\text{Mg}$  structures discussed before. In particular, the hyperfine modulation can be rationalized in terms of the presence of two nonequivalent  $^{17}\text{O}$  nuclei. In other words the structure of the spectrum reported in Figure 2a is not due to two distinct electron centers having different interaction with an oxygen neighbor ion but, rather, to a unique type of electron center interacting with two magnetically (and structurally) nonequivalent oxygen ions. This latter hypothesis is the only one compatible with the existence of the 36-line weak structure, which should not be present in the case of two different centers. This has been further checked through careful computer simulation that allows the precise identification of the spin Hamiltonian parameters. The simulation of the spectrum has been carried out on the basis of the following spin-Hamiltonian:

$$H = \mu_B g S + \sum \text{SAI} \quad (1)$$

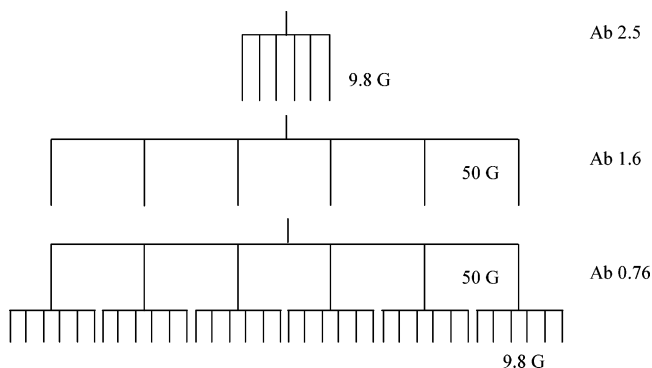
and is reported in Figure 2b. The simulation has been carried out using the same spin Hamiltonian parameters obtained in previous work<sup>4,16</sup> for the color centers generated on  $\text{Mg}^{16}\text{O}$  and adding the terms for the interaction with two different  $^{17}\text{O}$  nuclei. The complete set of the spin Hamiltonian parameters derived from the simulation is listed in Table 1 together with the data for the bulk defect studied by Allsop et al.<sup>17</sup>

**TABLE 1: Spin Hamiltonian Parameters for Surface Trapped Electrons on Polycrystalline MgO Derived from Computer Simulation**

species	Ab%	$g_{\parallel}$	$g_{\perp}$	H		$^{25}\text{Mg}$		$^{17}\text{O}$	
				$A_{\parallel}$ (G)	$A_{\perp}$ (G)	$A_{\parallel}$ (G)	$A_{\perp}$ (G)	$A_{\parallel}$ (G)	$A_{\perp}$ (G)
A	80	$2.0014 \pm 0.0002$	$1.9996 \pm 0.0002$	0.5	2.07	11.2	10.8	51.0	49.8
B	10	$2.001 \pm 0.002$	$1.999 \pm 0.002$	unres	unres	28	27	9.8	9.2
C	10	$2.001 \pm 0.002$	$1.999 \pm 0.002$	unres	unres	63	59	unres	unres
bulk <sup>a</sup>	-	$\langle g \rangle = 2.002$		-	5.2	3.8	7.0	3.9	unres

<sup>a</sup> From Allsop et al.<sup>17</sup>**TABLE 2: Theoretical  $a_{\text{iso}}$  Values (in G)<sup>a</sup>**

nuclide	(H <sup>+</sup> )(e <sup>-</sup> ) step	(H <sup>+</sup> )(e <sup>-</sup> ) reverse corner	(H <sup>+</sup> )(e <sup>-</sup> ) corner	$F_3(\text{H})^+$
$^{17}\text{O}$	-56.9 (1) -6.0 (3) $\approx -5$ (other O)	-28.5 (1) -18.3 (3) -9.3 (4)	-12.0 (1) -16.2 (3) -	-29.2 (1) -11.8 (3) $\approx -7$ (other O)
$^{25}\text{Mg}$	-14.9 (2) -1.5 (4)	-33.0 (2) -4.2 (5)	-60.0 (2) $\approx -1$ (other Mg)	-8.1 (2) -2.6 (4)
$^1\text{H}$	-4.3	-3.5	-2.0	-1.5

<sup>a</sup> The specified the atoms of each structure to which the computed value refers are in parentheses, see Figure 5.**SCHEME 1**

The electron center can be regarded as an unpaired electron interacting with two nonequivalent oxygen nuclei, ( $\text{O}_{\text{I}}(\text{e}^-)(\text{O}_{\text{II}})$ ). The unpaired electron has a relatively strong interaction with  $\text{O}_{\text{I}}$  and a weaker interaction with  $\text{O}_{\text{II}}$ . The first sextet (51 G) corresponds to the isotopomer having an ( $^{17}\text{O}_{\text{I}}(\text{e}^-)(^{16}\text{O}_{\text{II}})$ ) composition, the second one (9.8 G) is due to ( $^{16}\text{O}_{\text{I}}(\text{e}^-)(^{17}\text{O}_{\text{II}})$ ) and the 36-line structure to ( $^{17}\text{O}_{\text{I}}(\text{e}^-)(^{17}\text{O}_{\text{II}})$ ). The situation is graphically illustrated in the stick diagram of Scheme 1 where the abundance of each isotopomer, as deduced from the simulation, is also reported. Although this distribution of isotopomers seems to give the best fit of the experimental results, the possibility of having 3 oxygen nuclei, 2 of which (those with smaller constants at 9.8 G) magnetically equivalent, cannot be excluded on the basis of the simulation alone.

**3.b. Calculations.** Theoretical analysis of the spin densities has been performed for four distinct trapping electron sites whose importance arises from previous work of our groups.<sup>10,11,14,16</sup> The hfcc's for each of the four defects considered are reported in Tables 2 and 3. In particular, Table 2 reports the  $a_{\text{iso}}$  values for the  $^{17}\text{O}$ ,  $^{25}\text{Mg}$ , and  $^1\text{H}$  atoms nearest to the trapped electron, while Table 3 gives the  $A$  tensor for the  $^{17}\text{O}$  ions that exhibit the largest  $a_{\text{iso}}$  values.

On a MgO step the ( $\text{H}^+)(\text{e}^-)$  pair can give rise to two structures, (i) a symmetric configuration in which the OH bond is fixed in the direction perpendicular to the step line, Figure 4a, and (ii) an asymmetric configuration in which the H atom is tilted to one of the two nearby Mg ions. We find that the asymmetric configuration is more stable by 0.15 eV. That is, the symmetric configuration represents a transition state between

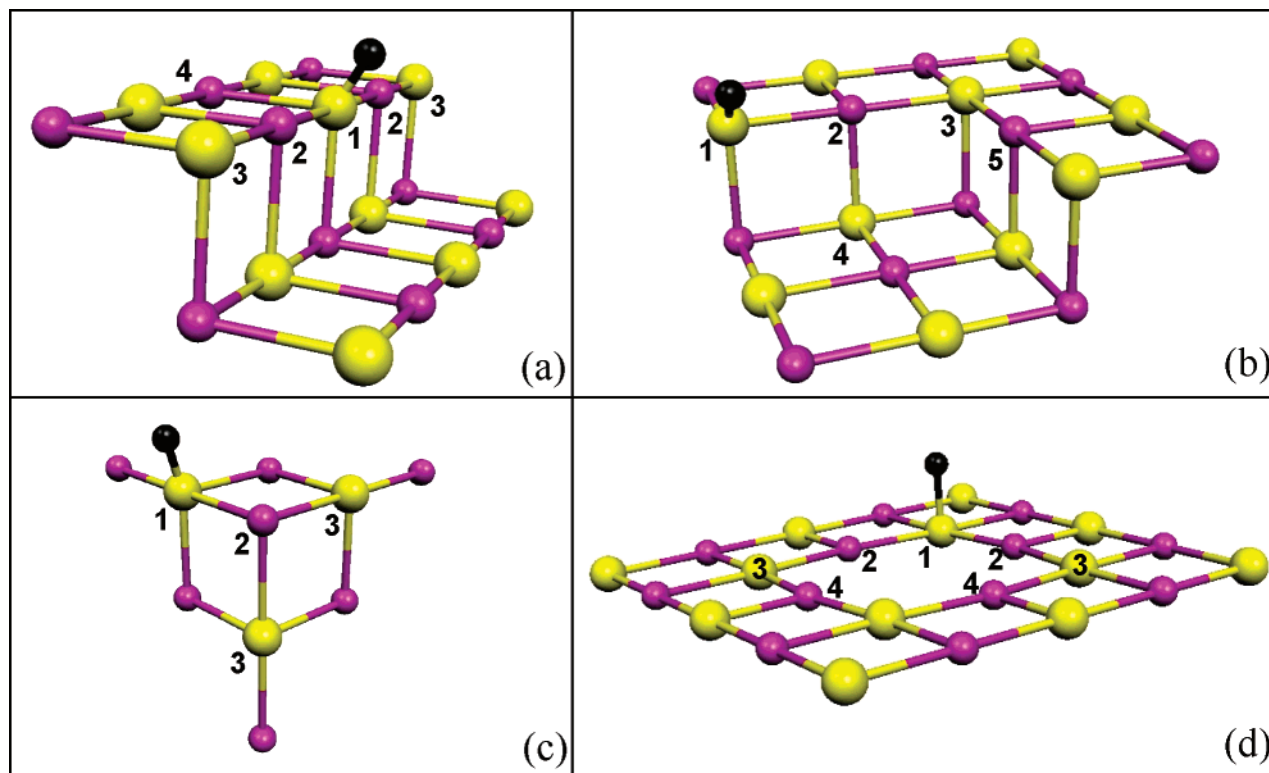
**TABLE 3: Complete Tensor for the  $^{17}\text{O}$  Atom Where the Proton Is Bound**

nuclide	(H <sup>+</sup> )(e <sup>-</sup> ) step	(H <sup>+</sup> )(e <sup>-</sup> ) reverse corner	(H <sup>+</sup> )(e <sup>-</sup> ) corner	$F_3(\text{H})^+$
$a_{\text{iso}}$	-56.9	-28.5	-12.0	-29.2
$B_1$	2.8	1.9	1.2	2.0
$B_2$	1.4	1.7	1.1	1.8
$B_3$	-4.2	-3.6	-2.3	-3.8
$A_1$	-54.1	-26.6	-10.8	-27.2
$A_2$	-55.5	-26.8	-10.9	-27.4
$A_3$	-61.1	-32.1	-14.3	-33.0

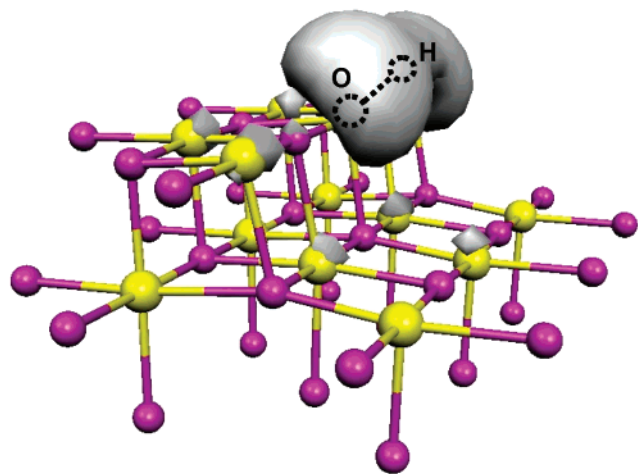
the two equivalent asymmetric configurations. However, as we discussed in detail,<sup>14</sup> the proton is very light as compared to the MgO and, because of the small barrier, it flips between the two tilted configurations so fast that the lattice cannot follow its motion. Instead, the lattice ions fluctuate near their positions, which corresponds to the average configuration of the OH bond, that is, the symmetric configuration. Thus, the potential energy surface for the OH bending has a single rather than double well profile.<sup>14</sup>

Figure 5 shows the spin density for this paramagnetic center. The spin is symmetrically distributed around the OH group, and largely localized on the two neighboring four-coordinated Mg cations. For this symmetric structure we found a high hfcc with the O atom directly bound to the proton, -57 G; the two  $\text{O}_{4c}$  neighbor ions exhibit  $a_{\text{iso}}$  values of -6 G. Smaller values are found on the other oxygens, Table 2. The  $a_{\text{iso}}$  for the two equivalent  $^{25}\text{Mg}$  ions is -15 G, with very small values on the remaining Mg ions. Finally, an  $a_{\text{iso}} = -4$  G is found for the H atom. The value of -57 G computed for  $^{17}\text{O}$  is close to that observed experimentally, 51 G (the sign cannot be established experimentally). Furthermore, the signal is highly isotropic, as shown by the small values of the dipolar part of the matrix, see Table 3, in full agreement with the observation for site A. Also  $a_{\text{iso}}(^{25}\text{Mg})$  is similar (although not identical) in theory and experiment, 15 G versus 11 G, respectively. Notice that smaller values, ( $\approx 13$  G for  $^{25}\text{Mg}$ ), have been reported in previous work using the less flexible 6-31G basis on the Mg ions.<sup>14</sup> The discrepancy between experimental and calculated values, however, is not dramatic for all nuclei ( $^{17}\text{O}$ ,  $^{25}\text{Mg}$ ,  $^1\text{H}$ ) so that, on this basis, it is tempting to assign the observed constants for species A to an electron trapped near a proton at an MgO step,  $\text{MgO}_{\text{step}}(\text{H}^+)(\text{e}^-)$ .





**Figure 4.** Schematic representation of the  $(H^+)(e^-)$  trapping sites at the MgO surface considered in this work for quantum mechanical modeling: (a) step, (b) reverse corner, (c) corner, and (d) oxygen vacancy on (100) terrace. White atoms: O; gray atoms: Mg; black atoms: H.



**Figure 5.** Spin density plot representing the unpaired electron trapped at the  $MgO_{step}(H^+)(e^-)$  site.

The  $^{17}O$  hyperfine structures for the minority sites B and C have not been resolved as they are probably buried in the dominating structure of the most abundant A site. Here we consider other possible but less abundant electron traps at the MgO surface and we concentrate on the corresponding  $^{17}O$  hfcc's. One possible site is the reverse corner, Figure 4b.<sup>14</sup> Here the proton is bound to an  $O_{4c}$  ion and the trapped electron is mostly localized on the Mg neighbor (see atom 2 in Figure 4b). The largest  $^{17}O$  hfcc is found for the O atom bound to the proton,  $-29$  G, while the O atom located at the intersection of the two steps, atom 3 in Figure 4b, has an  $a_{iso} = -18$  G. Finally, the O atom in the basal plane, atom 4, has an  $a_{iso} = -9$  G. Only the Mg ion nearest to the OH group exhibits a large hfcc,  $a_{iso} = -33$  G. A small  $a_{iso}$  of  $-4$  G is found on the other  $Mg_{4c}$  ion (see 5 in Figure 4b). The  $a_{iso}(^{25}Mg) = -33$  G is consistent with that measured for species B, Table 1.

The corner site is characterized by a proton bound to an  $O_{4c}$  ion with the electron trapped at the three-coordinated Mg ion, Figure 4c. This center can be viewed as an electron bound to a single Mg which becomes effectively  $Mg^{1+}$ .<sup>6</sup> This is reflected in the unusually high  $a_{iso}(^{25}Mg)$ , 60 G, but the corresponding  $a_{iso}(^{17}O)$  values are much smaller, 12 and 16 G, respectively (Table 2) and totally inconsistent with the value of 51 G deduced from the experiment. Furthermore, corner sites are certainly less abundant than steps, thus explaining why the  $^{17}O$  structure of this particular site has not been observed.

The centers considered so far belong to the "family" of  $(H^+)(e^-)$  pairs that have nothing in common with oxygen vacancies formed by removing an O ion from the lattice with consequent loss of local stoichiometry. Furthermore, while the  $MgO(H^+)(e^-)$  pairs are globally neutral,  $MgO$  anion vacancies with one trapped electron are charged. Here we consider the hyperfine interactions of one of these centers, the oxygen vacancy formed at a terrace site with a proton adsorbed in the vicinity, Figure 4d. The unpaired electron is trapped in the cavity formed between the first and the second layer of Mg and O ions. The presence of the proton polarizes the electron towards the OH group so that the distribution of hfcc's is asymmetric. The O ion bound to the proton has the largest  $a_{iso} = -29$  G, Table 2; this is considerably lower than that observed for species A, Table 1. The next largest  $a_{iso}(^{17}O)$ ,  $-12$  G, is associated with the two O ions at the border of the vacancy (see 3 in Figure 4d). The two Mg ions nearest to the OH group, see 2 in Figure 4d, have  $a_{iso}$  values of  $-8$  G, not too far from those reported for species A. Together with the fact that the  $a_{iso}$  for the proton,  $-1.5$  G, is very similar to the measured one, this prompted us to suggest some time ago that species A may be associated to electrons trapped in charged oxygen vacancies,  $F_5(H)^+$  centers.<sup>4</sup> This assignment has been questioned recently based on energetic as well as on other reasons.<sup>14</sup> Now, the direct measurement of

the  $^{17}\text{O}$  hfcc for species A, about 50 G, shows that the  $F_S(\text{H})^+$  center is incompatible with this value.

#### 4. Conclusions

In this study we have reported new EPR spectra of paramagnetic color centers formed on  $^{17}\text{O}$  enriched MgO samples. The enrichment of  $^{17}\text{O}$  was obtained by successive hydration and dehydration cycles of the MgO sample using  $\text{H}_2^{17}\text{O}$ . The isotopic substitution has been found to be a highly specific, site-selective process and demonstrates that the sites that are involved in electron-trapping phenomena are the same as those involved in the isotopic exchange process. Moreover, this facile exchange reaction based on hydration and dehydration cycles could be of great help in studying and elucidating the mechanism of oxides surface dehydration.

Based on  $^{17}\text{O}$  hyperfine coupling constants the nature of the local environment of the most abundant excess electron trapping site has been identified and assigned to morphological features present at steps present on the cubic microcrystal faces.

**Acknowledgment.** This work has been supported by the Italian Ministry of Research through a Cofin project. We thank P. Sushko and A. Shluger (London) for useful discussions and for making available the Guess code.

#### References and Notes

- (1) Schluman, J. H.; Compton, W. D. *Color Centers in Solids*; Pergamon Press: Oxford, 1962.
- (2) Matsuishi, S.; Toda, Y.; Miyakawa, M.; Hayashi, K.; Kamiya, T.; Hirano, M.; Tanaka, I.; Hosono, H. *Science* **2003**, *301*, 626.
- (3) Cernette, D. P.; Ichimura, A. S.; Aurbin, S.; Dye, J. L. *Chem. Mater.* **2003**, *15*, 1441.
- (4) Giamello, E.; Paganini, M. C.; Murphy, D. M.; Ferrari, A. M.; Pacchioni, G. *J. Phys. Chem. B*, **1997**, *101*, 971.
- (5) Chiesa, M.; Giamello, E.; Paganini, M. C.; Pacchioni, G.; Soave, R.; Murphy, D. M.; Sojka, Z. *J. Phys. Chem. B* **2001**, *105*, 497.
- (6) Chiesa, M.; Paganini, M. C.; Giamello, E.; Murphy, D. M.; Sojka, Z. *J. Chem. Phys. B* **2002**, *116*, 4266.
- (7) Feher, G. *Phys. Rev.* **1957**, *105*, 1122.
- (8) de Boer, J. H. *Recl. Trav. Chim.* **1937**, *56*, 301.
- (9) Sterrer, M.; Berger, T.; Diwald, O.; Knozinger, E. *J. Am. Chem. Soc.* **2003**, *125*, 195.
- (10) Murphy, D. M.; Yacob, A.; Purnell, I. J.; Farley, R. D.; Rowlands, C. C.; Paganini, M. C.; Giamello, E. *J. Phys. Chem. B* **1999**, *103*, 1944.
- (11) Paganini, M. C.; Chiesa, M.; Giamello, E.; Martra, G.; Coluccia, S.; Murphy, D. M.; Pacchioni, G. *Surf. Sci.* **1999**, *421*, 246.
- (12) Chiesa, M.; Paganini, M. C.; Giamello, E.; Murphy, D. *Langmuir* **1997**, *13*, 5306.
- (13) Diwald, O.; Hofmann, P.; Knözinger, E. *Phys. Chem. Chem. Phys.* **1999**, *1*, 713.
- (14) Ricci, D.; Di Valentin, C.; Pacchioni, G.; Sushko, P. V.; Shluger, A. L.; Giamello, E. *J. Am. Chem. Soc.* **2003**, *125*, 738.
- (15) Scorza, E.; Birkenheuer, U.; Pisani, C. *J. Chem. Phys.* **1997**, *107*, 9645.
- (16) Chiesa, M.; Paganini, M. C.; Giamello, E.; DiValentin, C.; Pacchioni, G. *Angew. Chem., Int. Ed.* **2003**, *42*, 1759.
- (17) Allsop, A. L.; Owen, J.; Hughes, A. E. *J. Phys. C* **1973**, *6*, L337.
- (18) Adamski, A.; Spalek, T.; Sojka, Z. *Res. Chem. Intermed.* **2003**, *29*, 793.
- (19) Becke, A. D. *J. Chem. Phys.* **1993**, *98*, 5648.
- (20) Lee, C.; Yang, W.; Parr, R. G. *Phys. Rev. B* **1988**, *37*, 785.
- (21) Weil, J. A.; Bolton, J. R.; Wertz, J. E. *Electron Paramagnetic Resonance*; John Wiley & Sons: New York, 1994.
- (22) Susko, P. V.; Shluger, A. L.; Catlow, C. R. A. *Surf. Sci.* **2000**, *450*, 153.
- (23) Franci, M. M.; Petro, W. J.; Hehre, W. J.; Binkley, J. S.; Gordon, M. S.; De Frees, D. J.; Pople, J. A. *J. Chem. Phys.* **1982**, *77*, 3654.
- (24) Hehre, W. J.; Ditchfield, R.; Pople, J. A. *J. Chem. Phys.* **1972**, *56*, 2257.
- (25) Barone, V. In *Recent Advances in Density Functional Methods, Part I*; Chong, D. P., Ed.; World Scientific: Singapore, 1996.
- (26) Pacchioni, G.; Frigoli, F.; Ricci, D.; Weil, J. A. *Phys. Rev. B* **2001**, *63*, 054102.
- (27) Frisch, M. J. et al. *Gaussian 98*, Revision A.6; Gaussian Inc.: Pittsburgh, PA, 1998.
- (28) Chiesa, M.; Paganini, M. C.; Giamello, E.; Di Valentin, C.; Del Vitto, A.; Pacchioni, G. to be published.